


Contrasting Pressure-Induced Metallization Processes in Layered Perovskites, α -Sr₂MO₄ ($M = \text{V}, \text{Cr}$)

Touru Yamauchi,^{1,*} Taku Shimazu,² Daisuke Nishio-Hamane,¹ and Hiroya Sakurai^{3,1}

¹*Material Design and Characterization Laboratory, Institute for Solid State Physics, University of Tokyo, 5-1-5 Kashiwanoha, Kashiwa, Chiba 277-8581, Japan*

²*Department of Physics, Graduate School of Science, Chiba University, 1-33 Yayoi-cho, Inage-ku, Chiba, Chiba 263-8522, Japan*

³*National Institute for Materials Science, 1-1 Namiki, Tsukuba, Ibaraki 305-0044, Japan*

 (Received 9 January 2019; revised manuscript received 18 June 2019; published 9 October 2019)

Electric resistivity, magnetic susceptibility, and x-ray diffraction measurements under high pressure are performed in both α -Sr₂VO₄ and α -Sr₂CrO₄, which are carefully prepared with regard to their stoichiometry. These measurements reveal contrasting and peculiar metallization processes of these compounds with increasing pressure. In contrast to a previously reported one in a V compound, we find two kinds of pressure-induced metallic states at low- ($T < 50$ K) and high-temperature ($T > 100$ K) regions. The high-temperature one seems to emerge beyond the pressure-induced Mott transition. The low-temperature one might imply a topological nature of the V compound, which is expected in the spin-orbit coupled $3d^1$ state that arises from their degenerated d_{zx} and d_{yz} orbitals.

DOI: [10.1103/PhysRevLett.123.156601](https://doi.org/10.1103/PhysRevLett.123.156601)

Both α -Sr₂VO₄ and α -Sr₂CrO₄ have an identical K₂NiF₄-type crystal structure. Isostructural La₂CuO₄, the mother compound of high- T_c cuprates, and Sr₂RuO₄, an exotic p -wave superconductor, are well known. α -Sr₂VO₄ has been an especially mysterious compound. There are various arguments about its electromagnetic states on both the experimental and theoretical sides [1–11]. Even though the magnetic system of this compound is considered to be a spin $s = 1/2$ square lattice, its ground state is still under debate [2–12]. Note that the electromagnetic properties of this compound are very sensitive to its off-stoichiometry [13]. With respect to α -Sr₂CrO₄, the situation is rather poor; namely, a small number of studies have appeared in the literature because high-quality bulk samples have only been first synthesized in recent years [14]. Let us extract a few physical aspects from these studies, which are commonly observed and/or widely accepted. (i) Stoichiometric compounds are strongly insulating [1,13,14]. (ii) Three (V) and two (Cr) kinds of phase transition appear at 0.0 GPa below 300 K [2–7,14]. (iii) The orbital degree of freedom is crucial [2–8,10]. These aspects are the starting points of this study.

Schematic K₂NiF₄-type structure is illustrated in an inset in Fig. 1(c). A space group $I4/mmm$ gives rise to a fourfold symmetry at M -ion sites ($M = \text{V}^{4+}, \text{Cr}^{4+}$), which causes d_{yz} and d_{zx} orbital degeneration. Both VO₆ and CrO₆ octahedra are elongated along the c axis. This results in splitting of the threefold degenerated t_{2g} orbitals into upper d_{xy} singlet and lower d_{yz} and d_{zx} doublet states, within the point charge model, as shown in an inset in Fig. 1(c) with a

notation of “ $M = \text{V}$.” In contrast to the V- $3d$ case, the negative charge-transfer-gap situation of Cr- $3d$ and O- $2p$ orbitals causes reversed singlet and doublet states, as shown in this figure with a notation “ $M = \text{Cr}$ ” [15]. These two kinds of electronic state lead to two expectations as follows: One is similar electronic conduction in the two compounds, since their highest occupied states, which mainly contribute to the electronic conduction, are the same. The other is different magnetic states arising from the existence (Cr) or absence (V) of a lower d_{xy} orbit, in which a spin $s = 1/2$ lies. Experimentally, similar optical conductivities [1] and different magnetic ground states [3,4,14] were observed.

Elaborate techniques to prepare stoichiometry finely tuned powder samples of α -Sr₂VO₄ and α -Sr₂CrO₄ have already appeared in the literature [4,14]. Submillimeter size single crystals of these two compounds can be obtained by injecting a small amount of pure H₂O into a gold capsule, which experiences heating and compressing processes when a precursor, orthorhombic β -type compound transforms to a tetragonal α -type one. The stoichiometry of these crystals can be checked by phase transition temperatures, which can be observed by magnetic susceptibility and electric resistivity measurements at ambient pressure. The high-pressure experiments to observe the electric resistivity (~ 14 GPa), the magnetic susceptibility (~ 2.2 GPa), and x-ray diffraction (~ 11 GPa) were carried out using a cubic-anvil-type, a piston-cylinder-type, and a diamond-anvil-type (DAC) pressure cell, respectively. Some detailed information for the pressure determination in these pressure cell is given in Supplemental Material [16]. Daphne oil (for $M = \text{V}$) or glycerol (Cr) was employed

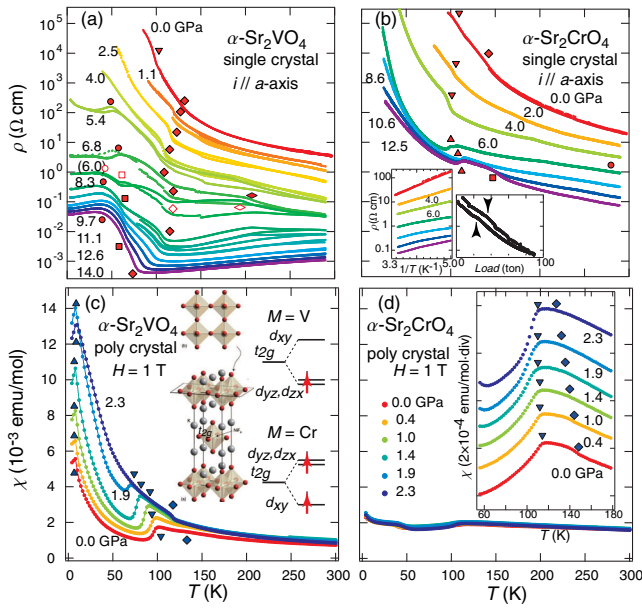


FIG. 1. (a) ρ - T curves under several pressures in α - Sr_2VO_4 . Several kinds of red symbol represent anomalies on the ρ - T curves. The closed (open) symbols denote the ρ - T curves measured in the loading (releasing) process. (b) Those in α - Sr_2CrO_4 . Two insets show an Arrhenius plot of the ρ - T curves above 200 K and the loading curves at 300 K, respectively. (c) χ - T curves under several pressures in the V compound. Several kinds of blue symbol represent anomalies on the χ - T curves. The inset shows a crystal structure and the schematic electronic states for both V and Cr compounds. (d) χ - T curves under several pressures in the Cr compound. The inset shows a macro graph of the χ - T curves around the two phase transitions.

as a pressure-transmitting medium [17]. The dc resistivity (ρ) of the single crystal was measured by the standard four-probe method with several dc-excitation currents running along the a axis. The dc susceptibility (χ) of the polycrystalline sample (~ 20 mg) was measured at an external magnetic field of 1.0 T, using a commercial magnetometer (MPMS-XL-7T, Quantum Design Co. Ltd.). In order to obtain precise χ , a large contribution from the pressure cell was subtracted from a raw output signal of the MPMS as explained previously [18]. The powder x-ray diffraction (XRD) profiles were observed by the backscattering method using an in-house x-ray source (Mo-rotor, RTPG-150, Rigaku Co. Ltd.) and a flat imaging plate (IP). Using Internet-distributed software, IPANALYZER and PDINDEXER [19], the observed XRD images are transformed into the one-dimensional profiles, and, from these profiles, we have evaluated the lattice constants a and c , the unit cell volume v , and the ratio a/c [20], assuming space group $I4/mmm$.

The pressure evolutions of temperature dependences of resistivity (ρ - T curves) are exhibited in Figs. 1(a) and 1(b) for α - Sr_2VO_4 and α - Sr_2CrO_4 , respectively. The several kinds of red symbol near the ρ - T curves such as the circle, square, diamond, etc., represent anomalies that could be accompanied with phase transitions. Note that the two

kinds of phase transition, which are already observed at ambient pressure and at around 100 K in both V and Cr compounds, appear as a slight kink and/or as a small hump of the ρ - T curves (solid symbols of diamond and inverted triangle). With increasing pressure (loading process), several kinds of additional anomalies appear (solid symbols of circle, square and rhombus in the V compound and solid symbols of triangle and square in the Cr compound). With decreasing pressure (releasing process), these anomalies are reversibly observed (open symbols of circle, square, diamond, and rhombus). The most significant observations are two kinds of metal-to-insulator transition (MIT) in the V compound. The first one is a MIT as a function of the pressure (P) at around 5–7 GPa. An appearance of this MIT in the pressure evolution of ρ - T curves is similar to that of iron-based ladder compound BaFe_2S_3 [21], in which a pressure-induced Mott transition contacts to a 24-K superconducting phase. Large hysteresis loops that appear in ρ - T curves between 5.4 and 6.8 GPa seem to be one manifestation of this pressure-induced MIT. The second one is a MIT as a function of the temperature (T) above 8 GPa at around 75–100 K (solid diamond). Furthermore, ρ - T curves above 8 GPa show a reentrant MIT at around 50 K (solid circle). In this reentrant low-temperature metallic phase, the absolute value of ρ is about 100 times larger than that in a usual high-temperature metallic phase. In contrast to the V compound, no MIT was found in the Cr compound. However, two kinds of phase transition previously reported at ambient pressure can be seen as two slight anomalies (solid symbols of inverted triangle and diamond) of the ρ - T curves. In addition to these, some pressure-induced anomalies (solid symbols of triangle, square, and circle) were also observed. Here, let us emphasize the following three differences between ρ - T curves below 4 and above 6 GPa. (i) An upward bending of the ρ - T curve at 100 K suddenly turns downward one (solid triangle \rightarrow solid inverted triangle). (ii) A pressure dependence of the slope of the ρ - T curve in the Arrhenius plot changes its tendency [left-hand side inset in Fig. 1(b)]. (iii) Both the loading and releasing curves (load dependences of ρ) at 300 K show a slight hump in between 4 and 6 GPa (upward and downward arrowheads in the right-hand side inset). These three aspects imply that a phase boundary lies vertically in the pressure-temperature (P - T) phase diagram at around 5 GPa.

The pressure evolutions of temperature dependences of susceptibility (χ - T curves) and anomalies on these curves (blue symbols) are also exhibited in Figs. 1(c) and 1(d) for V and Cr compounds, respectively. At first glance, very different pressure responses below 100 K between V and Cr compounds can be seen. This can be attributed to a peculiar magnetic state under 100 K, which has been debated in the V compound but not in the Cr compound [3,4,8]. Above 200 K, the absolute values of χ are twice different, probably owing to twice different numbers of spin sitting in V^{4+} and

in Cr^{4+} . These complementary χ - T observations cover invisible P - T regions in ρ measurements. For instance, the χ measurements clearly observed a magnetic transition at 8 K and at ambient pressure in the V compound (solid triangle), which could not be captured by ρ measurements because of its undetectable high resistivity. Naturally, two other transitions at 100 and 140 K can be seen on the χ - T curves of 0.0 GPa (solid symbols of inverted triangle and diamond for both V and Cr compounds). However, observed χ - T curves cannot yield any pressure-induced phase, which is observed in ρ measurements, because of the relatively lower capability of pressure generation (2.3 GPa) in the employed pressure cell. Additional discussions about the magnetic properties in the V compound, which has been under debate even at ambient pressure, are represented in Supplemental Material [16], which includes Refs. [22–31].

Combining the two kinds of result of ρ and χ measurements, we can draw the two P - T phase diagrams as shown in Fig. 2 for V and Cr compounds, respectively. The many kinds of blue (χ) and red (ρ) symbols shown in these phase diagrams have already appeared in Fig. 1. As shown in this figure, many phases emerge, and these phases will be represented by Roman numerals (I–VIII and I–VI for the V and Cr compound, respectively). All the phases observed at ambient pressure are naturally denoted by these numerals. The green and yellow regions show insulating and metallic phases, respectively. Let us focus on the phase diagram of the V compound. Two kind of MIT, as a function of T and that of P , result in a very complex P - T phase diagram. The first MIT, as a function of P , is represented as a hatched area in between 5 and 7 GPa with an end point at around 250 K in this phase diagram. Note that a loading curve of ρ at 300 K does not show any anomaly, in contrast to that of

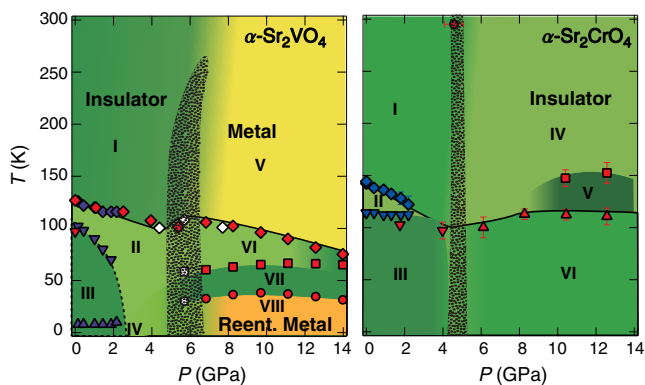


FIG. 2. Two P - T phase diagrams for $\alpha\text{-Sr}_2\text{VO}_4$ and $\alpha\text{-Sr}_2\text{CrO}_4$, deduced from electromagnetic measurements under pressure. The red (ρ) and blue (χ) symbols have already appeared in Fig. 1. The black hatched regions represent a MIT as a function of P in the V compound and a moderate insulator-insulator transition in the Cr compound (see the main text). Note that temperature-sweeping measurements find hard to capture a phase boundary that lies vertically in P - T phase diagrams. Green and yellow regions represent insulating and metallic phases, respectively.

the Cr compound. This implies the existence of an end point of this MIT, as discussed in Ref. [21]. This MIT is very clear at I \rightarrow V and II \rightarrow VIII phase transitions, but it is unclear at II \rightarrow VI and VII transitions because of the insulating natures in both the lower- and higher-pressure phases. The second MIT, as a function of T , is represented as red diamond symbols connected by a solid line, and the reentrant MIT is also shown by red circles. Additional discussions with regard to these pressure-induced metallic phases (V and VIII) and their electronic states are presented in Supplemental Material [16]. In contrast, no metallic region was observed in the Cr compound; thus, all the area of the phase diagram is colored in green. Furthermore, this compound never turns metallic up to 50 GPa [32].

Naively, one can expect that this contrast can be attributed to very soft or hard lattices against pressure. To check the pressure dependence of lattice constants, powder XRD profiles up to 11 GPa were observed at room temperature, and these results are exhibited in Fig. 3. In all panels of this figure, blue and red represent V and Cr compounds, respectively. Figures 3(a) and 3(b) show full XRD profiles under pressure, and the large drops of background levels at around $2\theta > 22^\circ$ are caused by the geometry of the DAC. As seen in these two panels, there is no major structural change in both the compounds, such as a tetragonal or orthorhombic structure change and/or enlarging of the unit cell, within an experimental resolution. The pressure dependences of normalized lattice constants a/a_0 and c/c_0 , where a_0 and c_0 are lattice constants observed at ambient pressure, are exhibited in

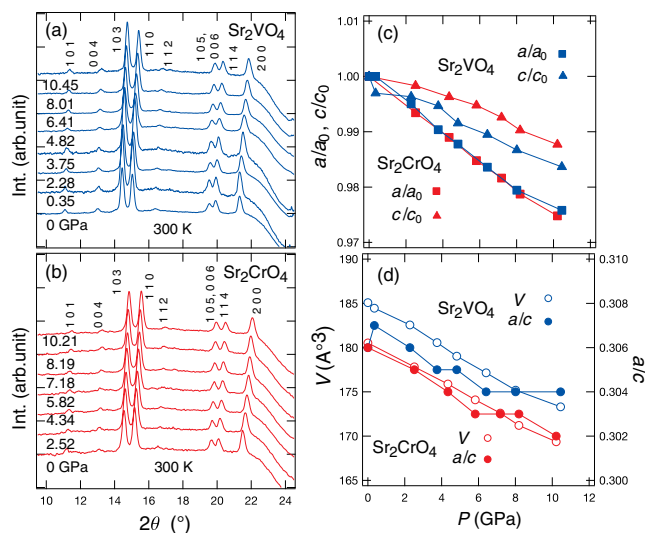


FIG. 3. In this figure, blue and red represent Sr_2VO_4 and Sr_2CrO_4 , respectively. (a) Powder x-ray diffraction profiles under several pressures in the V compound. (b) Those in the Cr compound. (c) Pressure dependences of normalized lattice constants a/a_0 and c/c_0 . a_0 and c_0 show values of a and c at ambient pressure, respectively. (d) Open circles show unit cell volume v (left axis), and filled circles denote a/c (right axis).

Fig. 3(c). Here, one can exclude a trivial scenario of very different bulk modulus for V and Cr compounds because of almost the same behaviors of a/a_0 against pressure, which is expected to be crucial for in-plane electronic conduction. Further detailed discussions are represented in Supplemental Material [16], including Rietvelt refinement of these XRD profiles.

Figure 3(d) shows pressure dependences of the unit cell volume v and the ratio a/c . Supplemental Material [16] gives the energetics of the V compound at controversial transitions observed at ambient pressure, using this $\delta v/\delta P$ and $\delta T_c/\delta P$, and suggests a non-Jahn-Teller origin of the transitions. It also shows that the elastic energy change of the unit cell can be evaluated as $\delta\epsilon \sim 0.5$ eV/f.u. for both V and Cr compounds, when 10 GPa is applied. Meanwhile, a typical energy difference between two phases with different orbital ordering patterns is calculated to be 0.02 eV/f.u. [15]. In this sense, the emergence of many kinds of phases, including the pressure-induced metallic state in the V compound (phase V), seems to be normal. Therefore, considering the absence of the metallic state in the Cr compound should be a first good step toward understanding high-pressure properties of these systems. One possible key is a peculiar electronic state in the Cr compound, which is schematically illustrated in the inset in Fig. 1(c). It consists of reverse splitting t_{2g} orbitals into lower d_{xy} singlet and higher d_{yz} and d_{zx} doublet states [15]. Very recent calculations yield that these d_{yz} and d_{zx} doublet states could retake the lower when the system is compressed [33]. As the most significant result of this, two $3d$ electrons in Cr^{4+} could lie together at the lower doublet states. This electronic state is expected to have a larger Hubbard U , which results in a more robust Mott insulating state against pressure. This retaking may also explain a vertical transition line drawn at around 4–6 GPa in the P - T phase diagram. Meanwhile, the Cr compound in this electronic state shall lose the orbital degree of freedom, which should be important in the discussions with regards to phases IV, V, and VI.

Finally, we touch the complex P - T phase diagram in the V compound. Note that it is evidently different from that shown in a previous work [34]. This difference is probably attributed to the sample (precisely stoichiometric crystal) and pressure (hydrostatic one) qualities. It is interesting to point out that a well-known schematic phase diagram for electronic materials, in which both electron correlation and spin-orbit coupling are non-negligible, might give an explanation for this P - T phase diagram. The schematic diagram is expanded between two parameters U/t and λ/t , where U , λ , and t denote Coulomb repulsion, spin-orbit coupling, and bandwidth, respectively (see Fig. 1 in Ref. [35]). As one can see in the literature [35,36], four kinds of phase—Mott insulator, simple metal, spin-orbit coupled insulator, and topological insulator (or semimetal)—contact each other. In 2009, Jackeli and Khaliullin proposed an octupolar ordered state in

phase III; namely, they claimed an emergence of spin-orbit coupled insulator at ambient pressure [8]. It should be noted that a recent theoretical study denies this octupolar scenario [12]. This corresponds to moving along the λ/t axis of the schematic diagram with a decreasing temperature. Meanwhile, this study shows a simple Mott transition (phase I \rightarrow V), which is a normal behavior in correlated electron systems; i.e., the system goes toward the origin of the schematic diagram (both U/t and λ/t decrease with compressing). Therefore, as a natural consequence from the schematic diagram, lowering the temperature above 8 GPa results in the appearance of a topological insulator phase (here, phases VI, VII, and VIII are approximately treated as a single phase). Note that the $\rho - T$ curves below the MIT and above 8 GPa (noted as “reentrant metal” in earlier parts of this Letter) have similar shapes with those in a typical topological insulator, $\text{Bi}_{2-x}\text{Sb}_x\text{Te}_{3-y}\text{Se}_3$ [37,38].

We observed enormously rich P - T phase diagrams in layered perovskites α - Sr_2VO_4 and α - Sr_2CrO_4 . The interplay between the electronic states (doublet or singlet ground state) and the orbital or spin degree of freedoms could be responsible for their complexity. To explicitly explain these phase diagrams, further precise crystal structure observations under high pressure, using single crystals and a synchrotron x-ray diffractometer, are desirable.

The authors thank Professor H. Ueda, Dr. J. Sugiyama, Professor H. Takahashi, and Professor Y. Ohta for valuable theoretical and experimental discussions. T. Y. also thanks, Professor Z. Hiroi, and Professor T. Ohama for educational management to a postgraduate student. This work was supported by Grants-in-Aid for Scientific Research (No. JP17K05531 and No. JP17K05521) from JSPS of Japan and by a JST-Mirai program (No. JPMJMI18A3) of Japan.

* yamauchi@issp.u-tokyo.ac.jp

- [1] J. Matsuno, Y. Okimoto, M. Kawasaki, and Y. Tokura, *Phys. Rev. Lett.* **95**, 176404 (2005).
- [2] J. Teyssier, E. Giannini, A. Stucky, R. Černý, M. V. Eremin, and D. van der Marel, *Phys. Rev. B* **93**, 125138 (2016).
- [3] I. Yamauchi, K. Nawa, M. Hiraishi, M. Miyazaki, A. Koda, K. M. Kojima, R. Kadono, H. Nakao, R. Kumai, Y. Murakami, H. Ueda, K. Yoshimura, and M. Takigawa, *Phys. Rev. B* **92**, 064408 (2015).
- [4] J. Sugiyama, H. Nozaki, I. Umegaki, W. Higemoto, E. J. Ansaldo, J. H. Brewer, H. Sakurai, T.-H. Kao, H.-D. Yang, and M. Månsson, *Phys. Rev. B* **89**, 020402(R) (2014); *J. Phys. Conf. Ser.* **551**, 012011 (2014).
- [5] M. V. Eremin, J. Deisenhofer, R. M. Eremina, J. Teyssier, D. van der Marel, and A. Loidl, *Phys. Rev. B* **84**, 212407 (2011).
- [6] J. Teyssier, R. Viennois, E. Giannini, R. M. Eremina, A. Günther, J. Deisenhofer, M. V. Eremin, and D. van der Marel, *Phys. Rev. B* **84**, 205130 (2011).

- [7] H. D. Zhou, Y. J. Jo, J. Fiore Carpino, G. J. Munoz, C. R. Wiebe, J. G. Cheng, F. Rivadulla, and D. T. Adroja, *Phys. Rev. B* **81**, 212401 (2010).
- [8] G. Jackeli and G. Khaliullin, *Phys. Rev. Lett.* **103**, 067205 (2009).
- [9] Y. Imai, I. Solovyev, and M. Imada, *Phys. Rev. Lett.* **95**, 176405 (2005).
- [10] H. D. Zhou, B. S. Conner, L. Balicas, and C. R. Wiebe, *Phys. Rev. Lett.* **99**, 136403 (2007).
- [11] H. Weng, Y. Kawazoe, X. Wan, and J. Dong, *Phys. Rev. B* **74**, 205112 (2006).
- [12] B. Kim, S. Khmelevskiy, P. Mohn, and C. Franchini, *Phys. Rev. B* **96**, 180405(R) (2017).
- [13] T. Ueno, J. Kim, M. Takata, and T. Katsufuji, *J. Phys. Soc. Jpn.* **83**, 034708 (2014).
- [14] Hiroya Sakurai, *J. Phys. Soc. Jpn.* **83**, 123701 (2014).
- [15] T. Ishikawa, T. Toriyama, T. Konishi, H. Sakurai, and Y. Ohta, *J. Phys. Soc. Jpn.* **86**, 033701 (2017).
- [16] See Supplemental Material at <http://link.aps.org/supplemental/10.1103/PhysRevLett.123.156601> for further deep discussions, which are elucidated from experimental data shown in a main text and from their analysis. It gives the magnetic, electronic, crystallographic, and energetic natures especially in V compound. Moreover, some detailed experimental information is also shown.
- [17] Sr_2VO_4 is chemically damaged in glycerol.
- [18] T. Yamauchi, H. Ueda, J.-I. Yamaura, and Y. Ueda, *Phys. Rev. B* **75**, 014437 (2007); T. Yamauchi, H. Ueda, K. Ohwada, H. Nakao, and Y. Ueda, *Phys. Rev. B* **97**, 125138 (2018).
- [19] http://pmsl.planet.sci.kobe-u.ac.jp/~seto/?page_id=23, http://pmsl.planet.sci.kobe-u.ac.jp/~seto/?page_id=20.
- [20] In addition to IPIndexer, we have also carried out Rietveld refinements using these XRD profiles. Details are exhibited in Supplemental Material [16].
- [21] T. Yamauchi, Y. Hirata, Y. Ueda, and K. Ohgushi, *Phys. Rev. Lett.* **115**, 246402 (2015).
- [22] H. Sakurai, *Phys. Procedia* **75**, 829 (2015).
- [23] J.-S. Zhou, J. B. Goodenough, and B. Dabrowski, *Phys. Rev. Lett.* **94**, 226602 (2005).
- [24] X. Obradors, L. M. Paulius, M. B. Maple, J. B. Torrance, A. I. Nazzari, J. Fontcuberta, and X. Granados, *Phys. Rev. B* **47**, 12353(R) (1993).
- [25] Y. Shimizu, H. Akimoto, H. Tsujii, A. Tajima, and R. Kato, *Phys. Rev. Lett.* **99**, 256403 (2007).
- [26] A. J. Millis, A. J. Schofield, G. G. Lonzarich, and S. A. Grigera, *Phys. Rev. Lett.* **88**, 217204 (2002).
- [27] T. Yamauchi and Y. Ueda, *Phys. Rev. B* **77**, 104529 (2008).
- [28] F. Izumi and K. Momma, *Solid State Phenom.* **130**, 15 (2007).
- [29] M. Cyrot, B. Lambert-Andron, J. L. Soubeyroux, M. J. Rey, P. H. Dehauht, F. Cyrot-Lackmann, and G. Fourcaudot, *J. Solid State Chem.* **85**, 321 (1990); T. Baikie, Z. Ahmada, M. Srinivasana, A. Maignanb, S. S. Pramanaa, and T. J. Whitea, *J. Solid State Chem.* **180**, 1538 (2007).
- [30] I. Loa, P. Adler, A. Grzechnik, K. Syassen, U. Schwarz, M. Hanfland, G. Kh. Rozenberg, P. Gorodetsky, and M. P. Pasternak, *Phys. Rev. Lett.* **87**, 125501 (2001).
- [31] T. Chatterji, F. Fauth, B. Ouladdiaf, P. Mandal, and B. Ghosh, *Phys. Rev. B* **68**, 052406 (2003).
- [32] H. Takahashi (private communication). Up to 50 GPa, no metallic behavior was observed. The phase transitions marked by a red triangle and square symbols as shown in Figs. 1 and 2 can be traced up to 40 GPa.
- [33] T. Yamaguchi, K. Sugimoto, and Y. Ohta (private communication). With regard to roughly estimated crystal structures under pressure from the powder XRD data shown in Fig. 3, GGA + U calculation reveals that d_{yz} and d_{zx} doublet states retake the bottom under appropriate U values.
- [34] S. Karmakar and Pallavi S. Malavi, *Phys. Rev. Lett.* **114**, 166402 (2015).
- [35] W. Witczak-Krempa, G. Chen, Y. B. Kim, and L. Balents, *Annu. Rev. Condens. Matter Phys.* **5**, 57 (2014).
- [36] S. Trebst, [arXiv:1701.07056v1](https://arxiv.org/abs/1701.07056).
- [37] T. Arakane, T. Sato, S. Souma, K. Kosaka, K. Nakayama, M. Komatsu, T. Takahashi, Z. Ren, K. Segawa, and Y. Ando, *Nat. Commun.* **3**, 636 (2012).
- [38] E. Frantzeskakis *et al.*, *Phys. Rev. B* **91**, 205134 (2015).